Computers and Electrical Engineering 100 (2022) 107871

Contents lists available at ScienceDirect

Computers and Electrical Engineering

journal homepage: www.elsevier.com/locate/compeleceng

Intelligent deep learning-enabled autonomous small ship detection and classification model

José Escorcia-Gutierrez [a,*], Margarita Gamarra [b], Kelvin Beleño [c], Carlos Soto [c], Romany F. Mansour [d]

[a] Electronics and Telecommunications Engineering Program, Universidad Autónoma del Caribe, Barranquilla, 08001, Colombia
[b] Departament of Computational Science and Electronic, Universidad de la Costa, CUC, Barranquilla, 08001, Colombia
[c] Mechatronics Engineering Program, Universidad Autónoma del Caribe, Barranquilla, 08001, Colombia
[d] Department of Mathematics, Faculty of Science, New Valley University, El-Kharga 72511, Egypt

ARTICLE INFO

Keywords:
Autonomous systems
Artificial intelligence
Ship detection
Deep learning
Mask RCNN
Parameter optimization

ABSTRACT

Autonomous ship technologies have gained considerable interest due to the minimization of the challenging issues faced by the unpredictable errors of manual navigation, and therefore reduces human labor, increasing navigation security and profit margin. On autonomous shipping technologies, small ship detection is vital in ensuring shipping safety. With this motivation, this paper presents an efficient optimal mask regional convolutional neural network (Mask-CNN) technique for small ship detection (OMRCNN-SHD) on autonomous shipping technologies. Primarily, the data augmentation process is performed to resolve the issue of the limited number of real-world samples of small ships and helps to detect small ships in most cases accurately. Besides, the Mask RCNN with SqueezeNet model is used to detect ships and the hyperparameter tuning of the SqueezeNet model takes place by the use of the Adagrad optimizer. Furthermore, the Colliding Body's Optimization (CBO) algorithm with the weighted regularized extreme learning machine (WRELM) technique is employed to classify detected ships effectively. The comparative results analysis demonstrates the betterment of the OMRCNN-SHD technique over the current methods with the maximum accuracy of 98.63%.

1. Introduction

The autonomous ship technique gradually changed and is rapidly developed from testing to the experimental stage. It can considerably decrease the problems caused by unexpected faults of manual navigation and consequently improve navigation security, promote the linked profit margins, and decrease human resources costs [1]. As it can be widely accepted that autonomous ships would be more appropriate for ocean navigation, many studies and applications focus on ship classification and recognition under marine environments [2]. Nevertheless, inland river navigation plays a vital role in water transportation despite ocean navigation. During the near-shore ocean or river environments, most compact targets, namely bamboo rafts and small fishing boats, and surface targets are small. This tiny target is complex, and discriminates against the challenging inland river environment, and frequently moves elusively within relatively narrow channels [3]. Hence, it is imperative to pay special attention to the applications of autonomous ships in

* Corresponding author: Electronic and Telecommunications Program, Universidad Autónoma del Caribe, Barranquilla, Atlántico, Colombia.
E-mail addresses: jose.escorcia23@gmail.com (J. Escorcia-Gutierrez), mgamarra3@cuc.edu.co (M. Gamarra), kelvin.beleno@uac.edu.co (K. Beleño), carlos.soto@uac.edu.co (C. Soto), romanyf@sci.nvu.edu.eg (R.F. Mansour).

https://doi.org/10.1016/j.compeleceng.2022.107871
Received 1 December 2021; Received in revised form 23 February 2022; Accepted 25 February 2022
Available online 3 March 2022

specific environments of inland rivers. Remarkably, the object identification in the channel is an essential part of safety control and navigation aids of autonomous ships. Ship detection through Synthetic Aperture Radar, surveillance video systems, and Satellite remote sensing (SAR) [4–8] gained considerable interest over the last few years, whereas the latter two could be applied directly in autonomous ships voyage.

With the development of AI technology, the deep learning (DL) technique [9] provides excellent strength for detecting SAR ship. According to the study [10], the DL method has nearly dominated the SAR ship detection communities for faster speed, less human intervention, higher accuracy, and suchlike. Hence authors are gradually employed DL-based ship detection performance in the field of study. In earlier stages, the DL method has been used in different parts of SAR ship detection, for example, ship discrimination land masking and region of interest (ROI) extraction (that is, ship or background binary classification of an individual chip). However, DL based SAR ship detection method uses an end-to-end mode to transmit SAR image to the network for the detection result [11]; without the help of auxiliary mechanisms (i.e., geoinformation, traditional pre-processing tools, among others) and without manual connection, the process of sea-land segmentation might require geoinformation to be removed, which significantly enhances detection performance. Additionally, the earth's coastline is changing continuously; hence the usage of coastline data in geodata lead to some deviation [12].

This paper presents an efficient optimal mask regional convolutional neural network (Mask-CNN) technique for small ship detection (OMRCNN-SHD) on autonomous shipping technologies. The OMRCNN-SHD technique involves the design of Mask RCNN with SqueezeNet model for the detection of ships, and the hyperparameter tuning of the SqueezeNet model takes place using the Adagrad optimizer. In addition, the colliding bodies optimization (CBO) algorithm with weighted regularized extreme learning machine (WRELM) technique is employed to classify detected ships effectively. The inclusion of Adagrad and CBO algorithms helps to optimally tune the parameters and thereby enhances the small ship classification performance. For exhibiting the improved outcomes of the OMRCNN-SHD technique, a series of experimental analyses is carried out, and the results are inspected under various aspects.

The rest of the paper is organized as follows Section 2. briefs the related works, Section 3 offers the proposed model, Section 4 validates the results, and Section 5 conclusions are summarized.

2. Related works

Guo et al [13]. presented a stable and effective single-stage detector named CenterNet++. This method primarily contains feature pyramids fusion, head enhancement, and feature refinement modules. First, We developed a feature refinement model to extract multiscale con-textual data to resolve small object detection problems. Next, the feature pyramids fusion model is designed to generate reliable semantic data. Chen et al [14]. focused on resolving the problem related to multi-object and small-object ship detection from complicated situations, for example, once a shipment reaches the port, suggesting a detection model based on an optimized feature pyramid network (FPN) technique. The feature pyramid module is first embedded from a conventional RPN and mapped to feature space for object recognition. Next, the k-means clustering approach-based shape similar distance (SSD) measure was utilized for optimizing the FPN.

Nina et al [15]. introduced a method that compares You Only Look Twice (YOLT) and YOLO on problems of small objects (ship) on optical satellite imagery. Two datasets have been utilized: Mini Ship Data Set (MSDS) and High-Resolution Ship Collection (HRSC). Jin et al [16]. developed a new lightweight patch-to-pixel CNN (P2P-CNN) to detect ships through PolSAR images. P2P-CNN aims at the surrounding and target. The appropriately sized patch comprising surroundings and target is employed as the NN input to determine the pixel in the center of the patch belonging to the target. Wang et al [17]. designed a small-scale ship detection method-based CNN algorithm. Firstly, redevelop the feature extraction system based on the character of ship targets from SAR image. The modified system could augment the semantics and spatial data of small ships. Next, proposed a PAFN for enhancing the fusion of distinct feature maps.

Devadharshini et al [18]. presented Hybrid YOLO's approach that realizes WordTree and K-Means Clustering for image classification and object identification. Also, Hybrid YOLO realizes SEPD to enhance ship targets and sea clutter and bounding box for network update. Liu et al [19]. projected a ship classification and detection method that employs the DCNN technique. The efficiency of the presented method was estimated on the group of images downloaded in Google Earth.

3. The proposed model

This study developed an effective OMRCNN-SHD technique to identify the small ships on autonomous shipping technologies. The OMRCNN-SHD technique aims to determine the occurrence of the small ships proficiently. Besides, the OMRCNN-SHD technique encompasses different stages, namely data augmentation, Mask RCNN with SqueezeNet based ship detection, Adagrad based hyperparameter tuning, Weighted Extreme Learning Machine (WELM) based classification, and CBO algorithm-based parameter optimization.

3.1. Data augmentation

Since the DL models require many images during the training process, it is necessary to increase the number of images from the dataset and thereby increase the classifier outcome. Therefore, data augmentation is used as a pre-processing stage. Then, the images are resized into a uniform size of 256×256 pixels for augmentation in various shifting methods such as right shift, image flipping, and left shift. Besides, the image flipping process transforms the right shift, pixel intensity, and left shift to modify the pixel's location to the right or left, respectively.

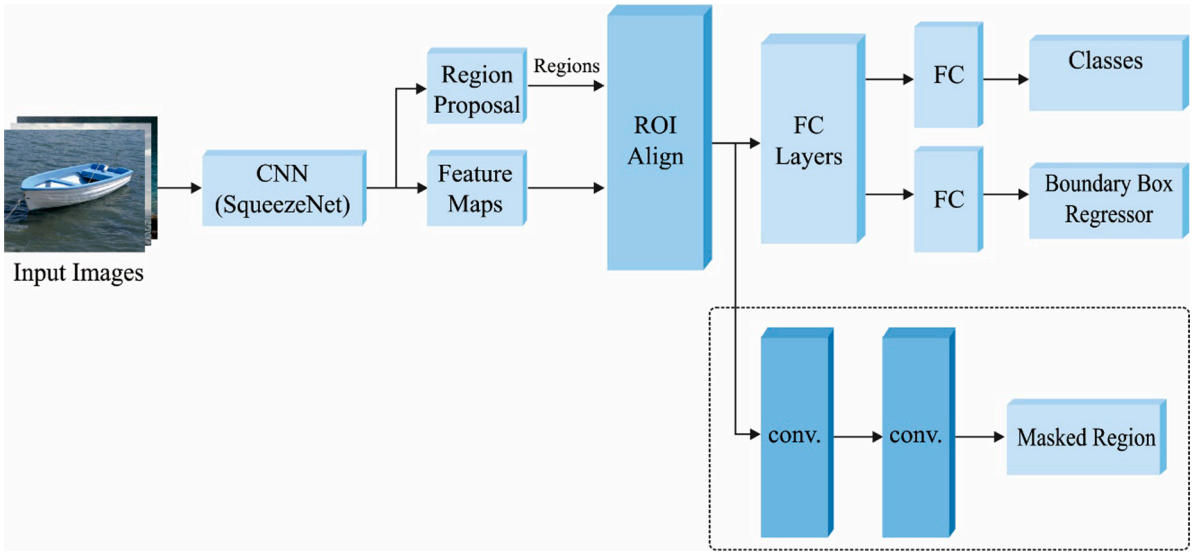

Fig. 1. Process involved in Mask RCNN based ship detection.

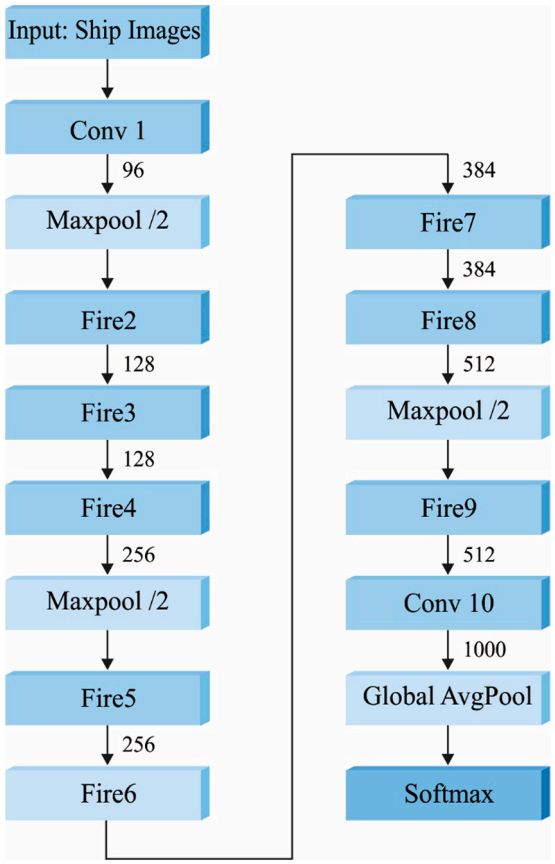

Fig. 2. Squeezet architecture.

3.2. Mask RCNN based ship detection

At this stage, the input images are passed into the Mask RCNN technique to detect small ships. In Mask R-CNN is a recent technique from the target detection domain, extending the target recognition structure of Faster R-CNN with more branch end of the model,

therefore attaining sample segmentation to all outcome proposal box utilizing FC layer. The segmentation is parallel with recognition and localized task. The Mask R-CNN structure is comprised of 3 steps [20]. Primarily, the backbone network removed feature maps in input the image. Secondary, feature map output from the backbone is sent to RPN for generating ROIs. Tertiary, ROIs output in RPN are mapped for extracting the equivalent target features from the shared feature map, and afterward, outcome to FC and FCN correspondingly, in order to target classifier and sample segmentation. This procedure created the classifier scores, bounding boxes, and segmentation masks Fig. 1. depicts the process involved in Mask RCNN based ship detection.

DNN techniques with various depths are introduced by designing distinct weight layers. Currently, VGG, AlexNet, GoogleNet, ResNet, or suchlike are the important techniques of DNN. Nevertheless, the deeper network may affect the superior accuracy, this technique's training and recognition speeds are diminished. As the remaining framework does not improve the model parameter, complexities of gradient disappearance and trained degradation are efficiently alleviated, and the convergence efficiency of the method is enhanced. Afterawards, the SqueezeNet was utilized as a backbone network to feature extraction.

Since the amount of VGGNet and AlexNet parameters are progressively improving, the SqueezeNet network is projected that is a small number of variables if continuing the accuracy. The Fire model is an essential technique from SqueezeNet [21], which is divided into Expand and Squeeze structures. The squeeze comprises a 1×1 convolution kernel. The Expand layer comprises a 3×3 convolutional kerneland a 1×1 kernel. The amount of 3×3 convolutional kernel is $E_{3 \times 3}$, and the amount of 1×1 convolutional kernel is $E_{1 \times 1}$. The module needs to fulfill $< (E_{1 \times 1} + E_{3 \times 3})$. Furthermore, the study describes in the perception of cross-channel pooling that MLP is similar to the cascaded cross-channel parametric pooling layer behindhand the classical convolution kernel, so obtaining a data integration across channels and linear integration of feature map Fig. 2. demonstrates the structure of Squeezet. The convolutional kernel becomes larger once the input and output networks are extensive. Hence, they add 1×1 convolutions to all the inception modules, reduce the number of input networks in the convolutional kernel parameter, and decrease the computational difficulty. Finally, a 1×1 convolution is added to improve feature extraction and channels. SqueezeNet changes 3×3 convolutional with 1×1 convolution to decrease the number of variables to one-ninth.

An image feature extraction was dependent upon shared convolutional layers. The fundamental network removes the low-level features like edge as well as angle. The high-level features which explain target forms are removed at a high level. For optimally representing the ship target on several scales, the FPN has been established to extend the backbone network that is particularly effective in recognizing small targets. The top-level features of the FPN structure are combined with fundamental features by upsampling through all layers individually forecasting feature maps.

3.3. Adagrad based hyperparameter tuning

The Adagrad optimizer allows tuning the hyperparameters of the Mask RCNN model through the calculation of the gradient and accumulating squared gradient of all parameters [22]:

$$G_t = \sum_{\tau=1}^{t} g_\tau \odot g_\tau \tag{1}$$

whereas $\odot$ represents an element-wise multiplication and $g_\tau \in \mathbb{R}^{|\theta|}$ denotes the gradient of the existing variables at the τ iteration. The upgrade values of the parameter in Adagrad is:

$$\Delta\theta_t = -\frac{\alpha}{\sqrt{G_t + \varepsilon}} \odot g_\tau \tag{2}$$

α represents the learning rate, and ε denotes a smoothing term that avoids division by zero. Since the rate of learning was predetermined beforehand training, as follows:

$$\Delta\theta_t = -\alpha\left(\frac{1}{\sqrt{G_t + \varepsilon}} \odot g_\tau\right) \tag{3}$$

From Eq. (2), G_t represents the preceding gradient. Consequently, the expression enclosed in parentheses could be viewed as one type of gradient revision as follows:

$$g_t^{'} = \frac{1}{\sqrt{G_t + \varepsilon}} \odot g_\tau \tag{4}$$

Therefore, the upgrade value of Adagrad is expressed by:

$$\Delta\theta_t = -\alpha g_t^{'} \tag{5}$$

It is analogous to the upgrade procedure of classical gradient descent. Hence, Adagrad is viewed as an optimization technique-based gradient.

3.4. Optimal WRELM based small ship classification

Next to the ship detection process, the next stage is to classify the small ships using the WRELM model. The WRELM was projected

to improve the typical ELM that utilizes the weight of all samples with non-parametric kernel density evaluation and defines the optimum weight to every instance [23]. Consider N hidden nodes from ELM and instance pair $\{X_i,P_i\}$, and the resultant of ELM was written as:

$$f(X_i) = \sum_{n=1}^{N} \alpha_n H(\varphi_n, X_i,\ b_n),\ \ i = 1, 2, \ldots, N, \tag{6}$$

where $H(\bullet)$ refers to the activation functions, ϕ_n signifies the input weight vectors, α_n signifies the n^{th} resultant weights, and b_n refers to equivalent biases.

$$\widetilde{P} = H\alpha = \begin{bmatrix} H(\varphi_1, X_1, b_1) & H(\varphi_2, X_1, b_2) & \cdots & H(\varphi_N, X_1, b_N) \\ H(\varphi_1, X_2, b_1) & H(\varphi_2, X_2, b_2) & \cdots & H(\varphi_N, X_2, b_N) \\ \vdots & \vdots & \vdots & \vdots \\ H(\varphi_1, X_N, b_1) & H(\varphi_2, X_N, b_2) & \cdots & H(\varphi_N, X_N, b_N) \end{bmatrix} \cdot \alpha, \tag{7}$$

where $\widetilde{P}$ stands for the resultant vectors, for obtaining the evaluation to the parameter α, the primary function was utilized as:

$$\text{argmin}\ \ \| \widetilde{P} - P \|_2^2 = \ \arg\min \| H\alpha - P \|_2^2, \tag{8}$$

where P implies the noticed data, the main purpose of weighted regularized ELM has written as:

$$\arg\min\ C \| \sigma\varepsilon \|_2^2 + \| \alpha \|_2^2 \tag{9}$$

dependent on the states,

$$P = H\alpha + \varepsilon \tag{10}$$

where σ signifies the diagonal matrix, ε refers to the vector of regression error, and C represents the regularization term. The Lagrange multipliers were established for solving the above-minimized issue, and the equivalent solution to α has provided as:

$$\alpha = \left(H^{'} \sigma^2 H + \frac{I}{C} \right)^{-1} H^{'} \sigma^2 P \tag{11}$$

The CBO algorithm can be applied to it optimally tune the weight and bias values of the WRELM model. The CBO algorithm is derived based on the similarity of collision laws among the objects [24]. A body can define every searching agent with velocity as well as mass. The primary location of the *ith* body is arbitrarily given in a *j*-dimension searching area defined by the users:

$$x_{ij} = x_{j,\ \min} + rand \cdot \left(x_{j,\ \max} - x_{j,\ \min} \right) \tag{12}$$

where rand indicates an arbitrary number in the range of [0, 1], the collision exists among two bodies, and the locations define the update depending upon the 1-dimension collision law. Provided a body X_k, the mass can be represented using Eq. (13):

$$m_k = \frac{1/J_k}{1/\sum_{i=1}^{n} (1/J_i)},\ \ k = 1,\ \ldots, n \tag{13}$$

where J_k indicates the cost function value of the *kth* particle and n that should be an even number, the n colliding bodies (CBs) are arranged in a rising way based on the objective function value, and they can be split into two equivalent sets such as stationary objects (SO) and moving objects (MO). The objects under the MO set collide with the SO set members for improving the location and shifting fixed objects in the direction of optimal locations. The collision pair is created based on the ascending order and objective function. The optimal moving particle is under collision with the optimal stationary particle. The velocity of the bodies prior to collision can be defined using Eqs. (13) and (15):

$$\text{Stationary body}: \ \ v_i = 0, i = 1, \frac{n}{2} \tag{14}$$

$$\text{Moving body}: \ \ v_j = x_{i-(n/2)} - x_i, i = \frac{n}{2} + 1, \ldots, n \tag{15}$$

Here, the velocity is undefined as the derivative of the location-based on time; however, it can be defined by the displacement in the searching area. Based on the colliding body theory, the velocity next to colliding bodies can be determined here.

$$\text{Stationary body}: v_i^{'} = \frac{\left(m_{i+(n/2)} + \varepsilon m_{i+(n/2)}\right) v_{i+(n/2)}}{m_i + m_{i+(n/2)}},\ \ i = 1, \ldots \frac{n}{2} \tag{16}$$

$$\text{Moving body}: v_i^{'} = \frac{\left(m_i - \varepsilon m_{i-(n/2)}\right) v_i}{m_i + m_{i-(n/2)}}, i = \frac{n}{2} + 1, \ldots n \tag{17}$$

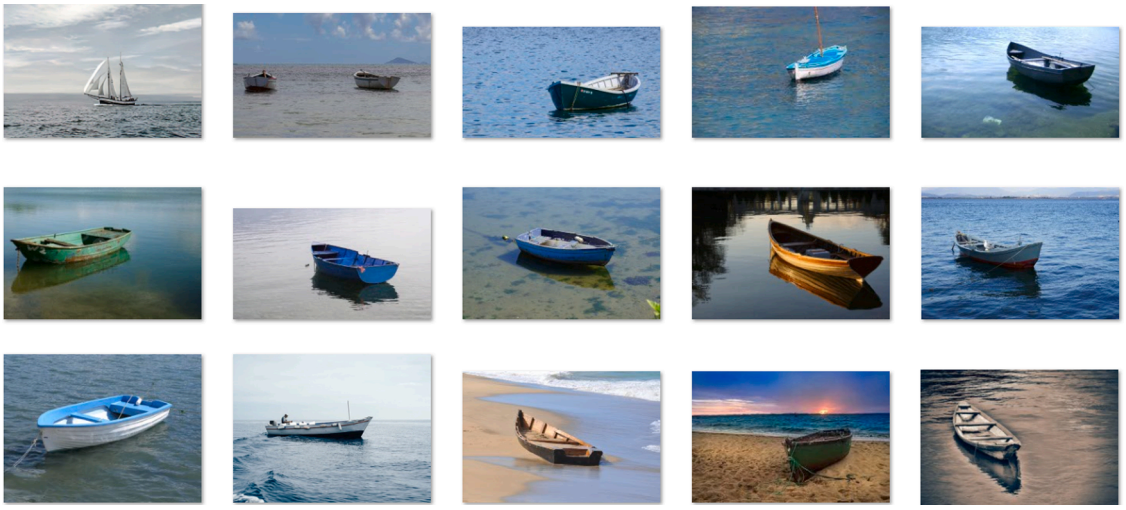

Fig. 3. Sample images.

where ε represents the coefficient of restitution and can be formulated using Eq. (18):

$$\varepsilon = \frac{\left|v_{i+1}^{'} - v_i^{'}\right|}{\left|v_{i+1} - v_i\right|} \tag{18}$$

The linear change from 1 to 1 is required during optimization, guaranteeing the trade-off between exploration and exploitation.. Once the displacement gets calculated, the next stage is to identify the new locations of the stationary as well as moving bodies using Eqs. (19) and (20):

$$\text{Stationary body}: \; x_i^{new} = x_j + rand \; .v_i^{'}, i = 1, \frac{n}{2} \tag{19}$$

$$\text{Moving body}: \; x_i^{new} = x_{i-(n/2)} + rand \; .v_i^{'}, i = \frac{n}{2} + 1, \ldots n \tag{20}$$

where rand implies an arbitrary vector under uniform distribution in the interval of [− 1, 1]. This iterative method, carried out on every particle at every round, continues until the termination condition is satisfied.

Pseudocode of CBO Algorithm

i. Initiation of CBO population in the searching area using Eq. (12).
ii. Determine the objective function and represent the mass using Eq. (13).
iii. Arrange the individual to identify the SO and MO groups and determine the velocity using Eqs. (14) and (15).
iv. Determine velocity followed by collisions using Eqs. (16) and (17).
v. The newly identified locations can be computed using Eqs. (18) and (19).
vi. When the stopping condition is satisfied, continue to step 7; otherwise, jump to step ii.
vii. Display the optimal solution obtained so far.
viii. End

The CBO technique resolves the FF for attaining enhanced classifier efficiency. It is defined as a positive integer representing the optimum efficiency of the candidate solution. The minimized classifier error rate was regarded as FF during this case, as offered in Eq. (21). An optimal solution is a lesser error rate, and the worst solution gains a higher error rate.

$$\begin{aligned} &fitness(x_i) = Classifier\ Error\ Rate(x_i) \\ &= \frac{numerb\ of\ misclassified\ images}{Total\ number\ of\ images} * 100 \end{aligned} \tag{21}$$

4. Experimental validation

The performance validation of the OMRCNN-SHD technique takes place using Python 3.6.5. tool. We have collected a dataset comprising 250 ship images and 1000 non-ship images. The OMRCNN-SHD technique performs data augmentation differently (as defined in Section 3.1), and the number of augmented images under shop class becomes 750. A few sample images are illustrated in Fig. 3.

Fig. 4 illustrates the sample set of small ship detection images. The figure revealed that the OMRCNN-SHD technique has the ability to accomplish the maximum detection rate on all the ships existing in the test images. It is also noticed that the OMRCNN-SHD

Fig. 4. Visualization of sample small ship detection images.

Table 1
Result analysis of OMRCNN-SHD technique with different measures.

Dataset Size	Precision	Recall	Accuracy	F-Score	MCC
Training/Testing - 80:20	98.60	98.90	98.75	98.75	97.50
Training/Testing - 70:30	98.41	98.80	98.60	98.60	97.20
Training/Testing - 60:40	98.40	98.70	98.55	98.55	97.10
Average	**98.47**	**98.80**	**98.63**	**98.63**	**97.27**

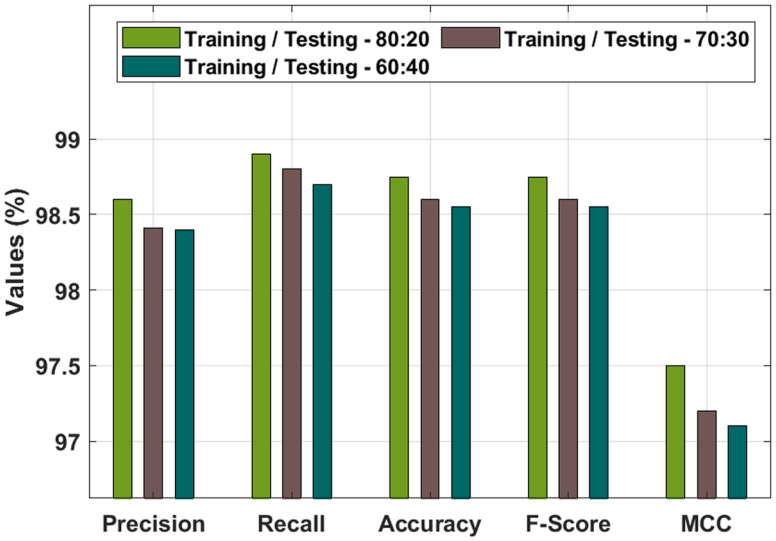

Fig. 5. Result analysis of OMRCNN-SHD technique.

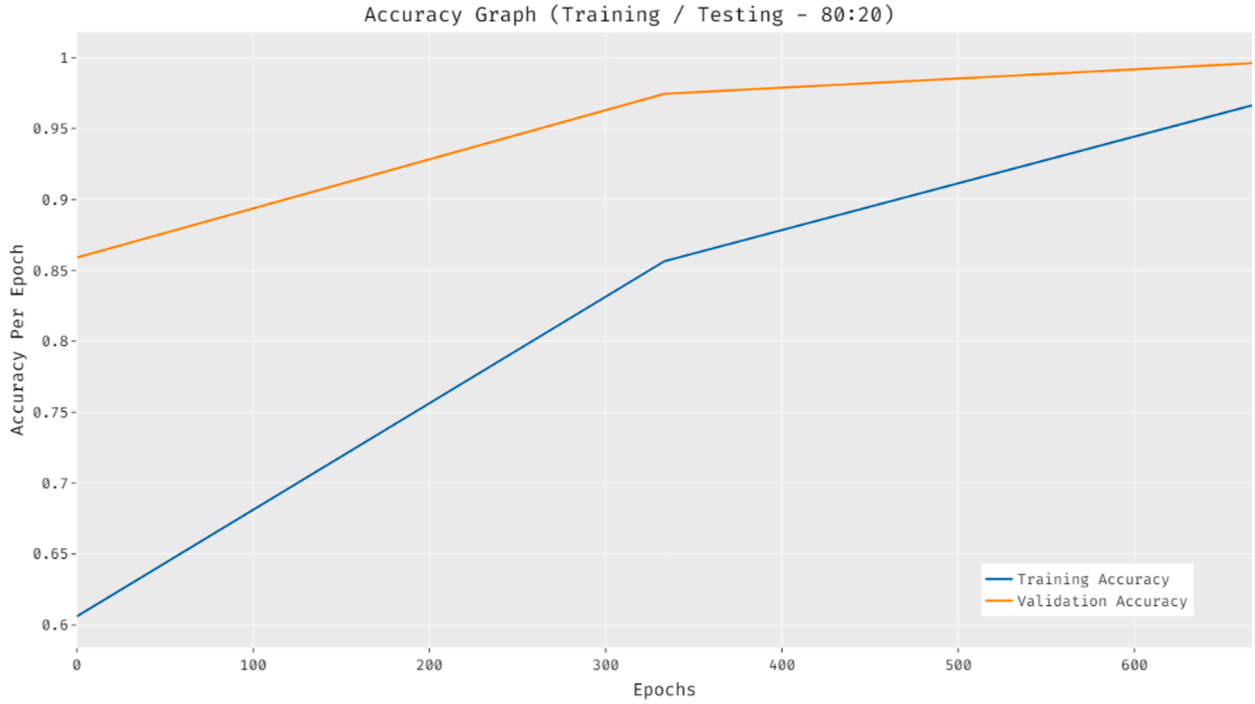

Fig. 6. Accuracy analysis of OMRCNN-SHD approach on training/testing (80:20).

technique has effectively masked the ship regions in the images.

Table 1 and Fig. 5 outlies the ship detection performance of the OMRCNN-SHD technique under varying sizes of training/testing data. The results show that the OMRCNN-SHD technique can obtain effective classification outcomes under all training/testing data. For instance, with training/testing data of 80:20, the OMRCNN-SHD technique has gained precision of 98.60%, recall of 98.90%, accuracy of 98.75%, F-score of 98.75%, and MCC of 97.50%. Similarly, with training/testing data of 70:30, the OMRCNN-SHD algorithm has reached precision of 98.41%, recall of 98.80%, accuracy of 98.65%, F-score of 98.60%, and MCC of 97.20%. Likewise, with training/testing data of 60:40, the OMRCNN-SHD method has attained precision of 98.40%, recall of 98.70%, accuracy of 98.55%, F-score of 98.55%, and MCC of 97.10%.

Fig. 6 illustrates the accuracy analysis of the OMRCNN-SHD approach on training and testing (80:20) dataset. The outcomes exhibited that the OMRCNN-SHD manner has enhanced performance with maximum training and validation accuracy. It can be stated

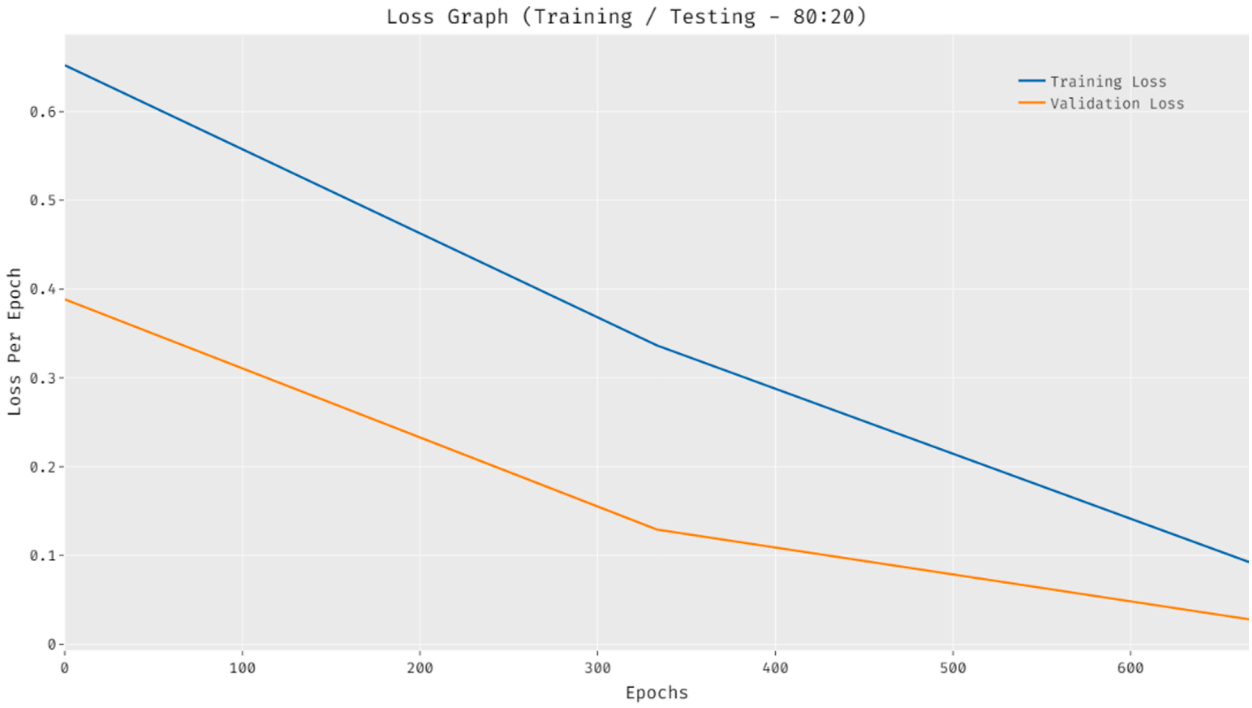

Fig. 7. Loss analysis of OMRCNN-SHD approach on training/testing (80:20).

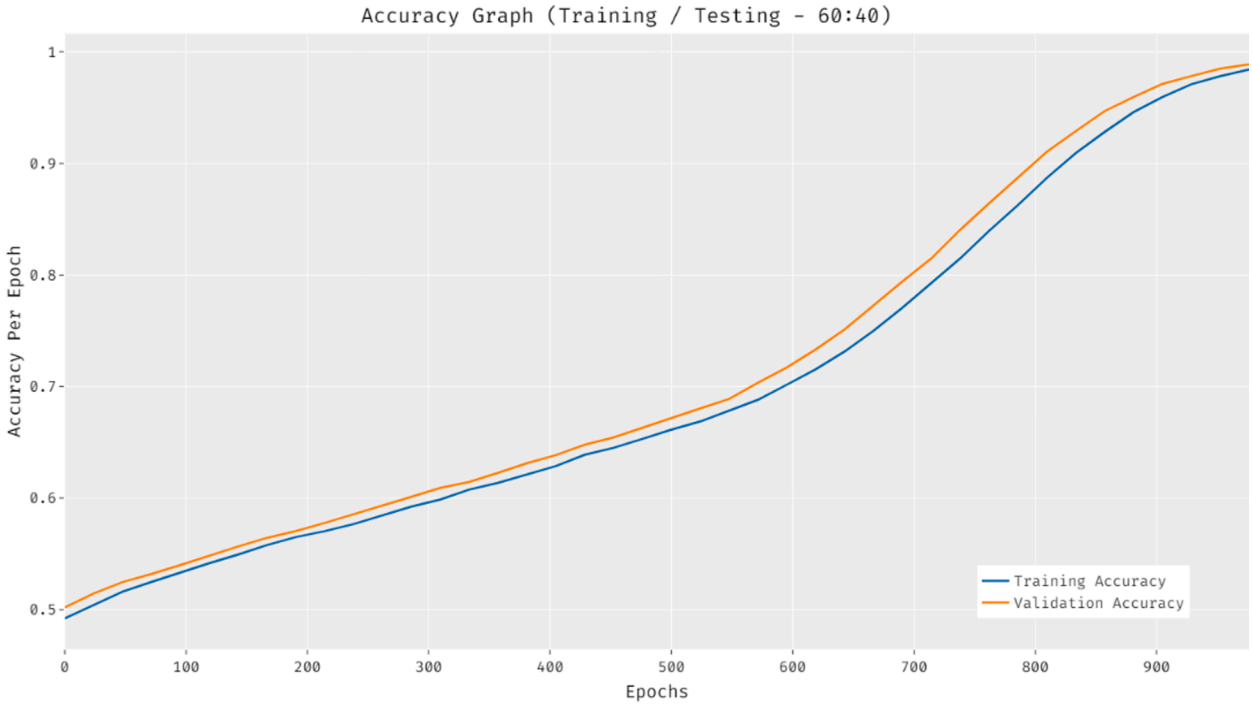

Fig. 8. Accuracy analysis of OMRCNN-SHD approach on training/testing (60:40).

that the OMRCNN-SHD approach has reached maximum validation accuracy on the training accuracy.

Fig. 7 showcases the loss analysis of the OMRCNN-SHD method on training and testing (80:20) dataset. The outcomes introduced that the OMRCNN-SHD approach has resulted in a proficient outcome with the lower training and validation loss. Obviously, the OMRCNN-SHD approach has obtainable lower validation loss on the training loss.

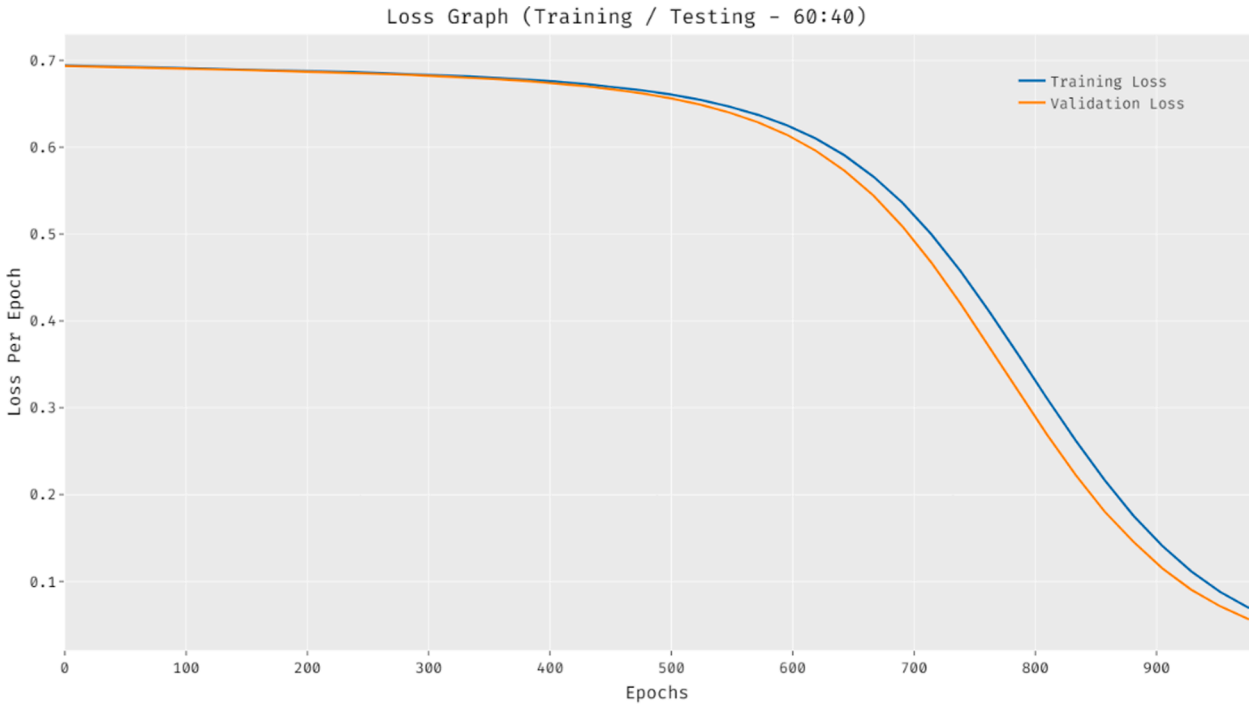

Fig. 9. Accuracy analysis of OMRCNN-SHD approach on training/testing (60:40).

Table 2
Comparative analysis of OMRCNN-SHD approach with existing methods.

Method	Accuracy	TPR	FPR
FR-CNN Model	86.00	96.00	24.00
SSD Model	93.00	94.00	8.00
YOLO v2	91.00	92.00	2.00
SSD-WGAN-GP	94.00	94.00	6.00
YOLO v2-DCGAN	94.00	90.00	4.00
DL-ASSD	97.00	98.00	3.00
OMRCNN-SHD	98.63	98.80	1.53

Fig. 8 displays the accuracy analysis of the OMRCNN-SHD technique on training and testing (60:40) dataset. The outcomes outperformed that the OMRCNN-SHD system's enhanced performance with maximal training and validation accuracy. It can be clear that OMRCNN-SHD methodology has reached maximal validation accuracy on the training accuracy.

Fig. 9 demonstrates the loss analysis of the OMRCNN-SHD approach on training and testing (60:40) dataset. The outcomes introduced that the OMRCNN-SHD approach has resulted in a proficient outcome with the lower training and validation loss. It is revealed that the OMRCNN-SHD system has obtainable lower validation loss on the training loss.

Table 2 depicts the comparative ship detection result analysis of the OMRCNN-SHD technique with current methods.

Fig. 10 illustrates the accuracy analysis of the OMRCNN-SHD method with other systems. The figure showcased that the FR-CNN algorithm has accomplished the minor performance with the minimal accuracy of 86%. Concurrently, the SSD, YOLOv2, SSD-WGAN-GO, and YOLO v2-DCGAN techniques have demonstrated slightly improved accuracy of 93%, 91%, 94%, and 94%, respectively. Simultaneously, the DL-ASSD technique has tried to exhibit considerable performance with an accuracy of 97%. However, the OMRCNN-SHD technique has illustrated enhanced outcomes with an accuracy of 98.63%.

Fig. 11 showcases the TPR analysis of the OMRCNN-SHD approach with other algorithms. The figure portrayed that the YOLO v2-DCGAN method has accomplished worse performance with a reduced TPR of 90%. Along with that, the YOLOv2, SDD, SSD-WGAN-GO, and FR-CNN methodologies have outperformed somewhat increased TPR of 92%, 94%, 94%, and 96% correspondingly. Also, the DL-ASSD algorithm has tried to showcase many performances with a TPR of 98%. At last, the OMRCNN-SHD algorithm has outperformed increased results with a TPR of 98.80%.

A brief FPR analysis of the OMRCNN-SHD technique with recent approaches is provided in Fig. 12. The figure shows that the FR-CNN model results in a maximum FPR of 24%. In line with this, the SSD, SSD-WGAN-GO, and YOLO v2-DCGAN techniques have reached certainly decreased FPR of 8%, 6%, and 4%, respectively. Followed by, the YOLO v2 and DL-ASSD techniques have accomplished reasonable FPR of 2% and 3%, respectively. However, the OMRCNN-SHD technique has outperformed the other

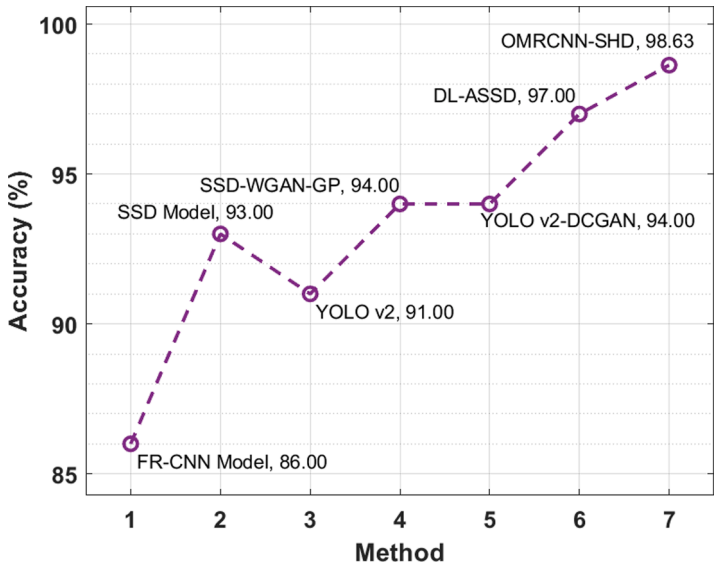

Fig. 10. Accuracy analysis of OMRCNN-SHD approach with recent methods.

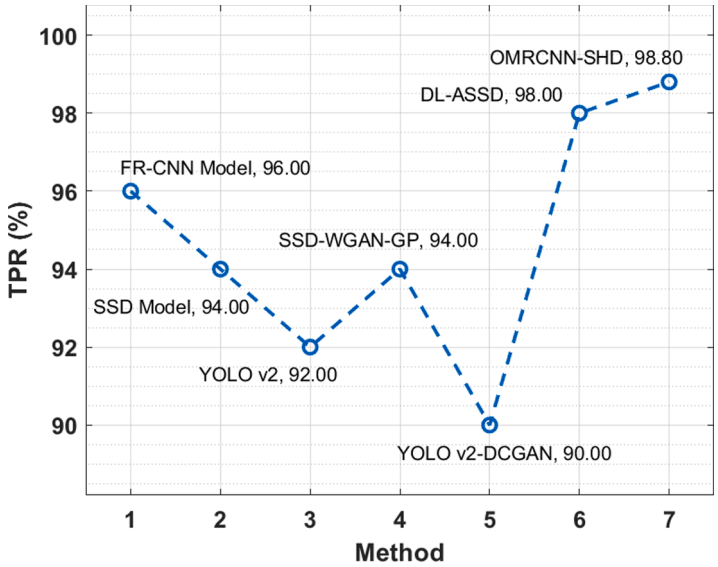

Fig. 11. TPR analysis of OMRCNN-SHD approach with recent methods.

methods with a minimal FPR of 1.53%.

Finally, a computation time (CT) analysis of the OMRCNN-SHD method occurs in Table 3 and Fig. 13. The results reported that the SSD and SSD-WGAN-GP techniques had offered higher CTs of 110s and 99s, respectively. At the same time, the YOLOv2 and YOLO v2-DCGAN techniques have obtained moderate CT of 89s and 80s, respectively. Moreover, the FR-CNN and DL-ASSD techniques have reached near-optimal CT of 67s and 59s, respectively. However, the OMRCNN-SHD technique has accomplished an effective CT of 31s. These results and discussion show that the OMRCNN-SHD technique can be employed for accurate small ship detection and classification.

5. Conclusion

This study has developed an effective Optimal Mask Regional Convolutional Neural Network technique for small ship detection to identify the small ships on autonomous shipping technologies. The forenamed technique aims to determine the occurrence of the small ships proficiently. Besides, it technique encompasses different stages: data augmentation, Mask Region-Based Convolutional Neural Network with SqueezeNet based ship detection, Adagrad based hyperparameter tuning, Weighted Extreme Learning Machine based

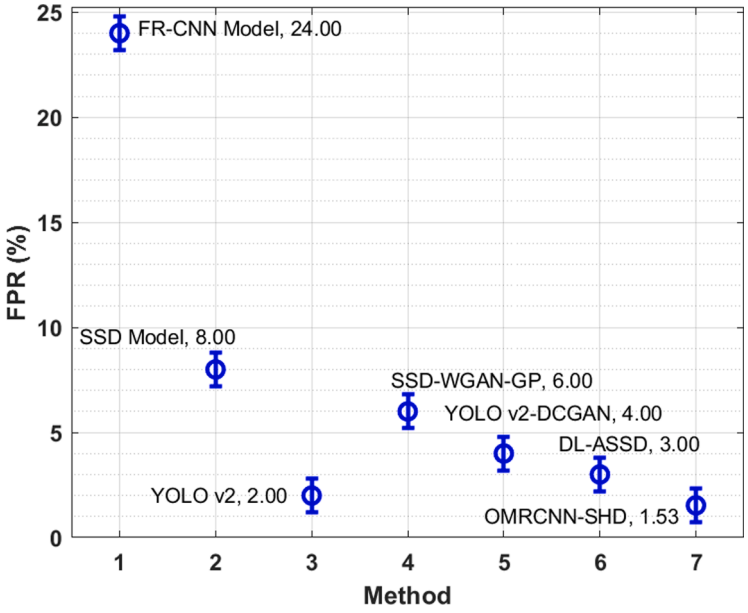

Fig. 12. FPR analysis of OMRCNN-SHD approach with recent methods.

Table 3
CT analysis of OMRCNN-SHD approach with existing methods.

Method	Computation Time (sec)
SSD Model	110.00
SSD-WGAN-GP	99.00
YOLO v2	89.00
YOLO v2-DCGAN	80.00
FR-CNN Model	67.00
DL-ASSD	59.00
OMRCNN-SHD	31.00

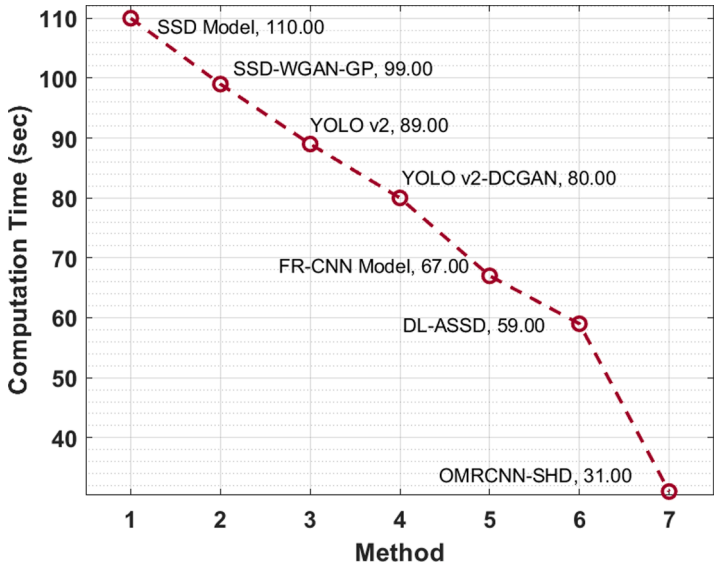

Fig. 13. CT analysis of OMRCNN-SHD method with existing algorithms.

classification, and Colliding Body's Optimization algorithm-based parameter optimization including Adagrad helps to optimally tune the parameters and thereby enhances the small ship classification performance. The SqueezeNet model is employed as a baseline model for Mask Region-Based Convolutional Neural Network. The design of effective hyperparameter optimizers assists in accomplishing maximum classification performance. To showcase the superior performance of the proposed technique, a wide range of simulations occur, and the outcomes demonstrate the betterment over the recent techniques with a maximum accuracy of 98.63%. Therefore, the proposed model can be employed for accurate small ship detection and classification. Future works will enhance the Optimal Mask Regional Convolutional Neural Network technique using hybrid Deep Learning-based ship detection methods.

Declaration of Competing Interest

The authors declare that they have no conflict of interest. The manuscript was written through contributions of all authors. All authors have given approval to the final version of the manuscript.

Data availability statement

Data sharing not applicable to this article as no datasets were generated during the current study.

Ethics approval

This article does not contain any studies with human participants performed by any of the authors.

Consent to participate

Not applicable.

References

[1] Chen Z, Chen D, Zhang Y, Cheng X, Zhang M, Wu C. Deep learning for autonomous ship-oriented small ship detection. Saf Sci 2020;130:104812.
[2] Tran T, Le T. Vision based boat detection for maritime surveillance. In: International Conference on Electronics, Information, and Communications. IEEE; 2016. p. 1–4.
[3] Wackerman CC, Friedman KS, Pichel WG, Clemente-Col ONP, Li X. Automatic detection of ships in RADARSAT-1 SAR imagery. Can J Remote Sens 2001;27(5):568–77.
[4] Wijnhoven R, van Rens K, Jaspers EG, de With PH. Online learning for ship detection in maritime surveillance. In: Procceedings of 31th Symposium on Information Theory in the Benelux; 2010. p. 73–80.
[5] Yang X, Sun H, Fu K, Yang J, Sun X, Yan M, Guo Z. Automatic ship detection in remote sensing images from google earth of complex scenes based on multiscale rotation dense feature pyramid networks. Remote Sens 2018;10(1):132.
[6] Mansour R, Escorcia-Gutierrez J, Gamarra M, Villanueva J, Leal N. Intelligent video anomaly detection and classification using faster RCNN with deep reinforcement learning model. Image Vision Comput 2020;112:104229.
[7] Zurek E, Gamarra M, Escorcia-Gutierrez J, Gutierrez C, Bayona H. A robust application in vessel recognition based on neural classification of acoustic fingerprint. Int J Artif Intell 2018;16(1):195–213.
[8] Yao Y, Jiang Z, Zhang H, Zhao D, Cai B. Ship detection in optical remote sensing images based on deep convolutional neural networks. J Appl Remote Sens 2017;11(4):042611.
[9] Zhang X, Wang H, Xu C, Lv Y, Fu C, Xiao H, He Y. A lightweight feature optimizing network for ship detection in SAR image. IEEE Access 2019;7:141662–78.
[10] Fan Q, Chen F, Cheng M, Lou S, Xiao R, Zhang B, Wang C, Li J. Ship detection using a fully convolutional network with compact polarimetric SAR images. Remote Sens 2019;11:2171.
[11] Fu J, Sun X, Wang Z, Fu K. An anchor-free method based on feature balancing and refinement network for multiscale ship detection in SAR images. IEEE Trans Geosci Remote Sens 2020.
[12] Fu J, Sun X, Wang Z, Fu K. An anchor-free method based on feature balancing and refinement network for multiscale ship detection in SAR images. IEEE Trans Geosci Remote Sens 2020.
[13] Guo H, Yang X, Wang N, Gao X. A CenterNet++ model for ship detection in SAR images. Pattern Recognit 2021;112:107787.
[14] Chen P, Li Y, Zhou H, Liu B, Liu P. Detection of small ship objects using anchor boxes cluster and feature pyramid network model for SAR imagery. J Mar Sci Eng 2020;8(2):112.
[15] Nina W, Condori W, Machaca V, Villegas J, Castro E. Small ship detection on optical satellite imagery with YOLO and YOLT. In: Future of Information and Communication Conference. Cham: Springer; 2020. p. 664–77.
[16] Jin K, Chen Y, Xu B, Yin J, Wang X, Yang J. A patch-to-pixel convolutional neural network for small ship detection with PolSAR Images. IEEE Trans Geosci Remote Sens 2020;58(9):6623–38.
[17] Wang J, Lin Y, Guo J, Zhuang L. SSS-YOLO: towards more accurate detection for small ships in SAR image. Remote Sens Lett 2021;12(2):93–102.
[18] Devadharshini S, Kalaipriya R, Rajmohan R, Pavithra M, Ananthkumar T. Performance investigation of Hybrid YOLO-VGG16 based ship detection framework using SAR images. In: 2020 International Conference on System, Computation, Automation and Networking (ICSCAN). IEEE; 2020. p. 1–6.
[19] Liu Y, Cui HY, Kuang Z, Li GQ. Ship detection and classification on optical remote sensing images using deep learning. In: ITM Web of Conferences. EDP Sciences; 2017. p. 05012. Vol. 12.
[20] Yu Y, Zhang K, Yang L, Zhang D. Fruit detection for strawberry harvesting robot in non-structural environment based on Mask-RCNN. Comput Electron Agric 2019;163:104846.
[21] Xu Y, Yang G, Luo J, He J. An Electronic component recognition algorithm based on deep learning with a faster squeezeNet. Math Probl Eng 2020:2020.
[22] Zhang C, Yao M, Chen W, Zhang S, Chen D, Wu Y. Gradient descent optimization in deep learning model training based on multistage and method combination strategy. In: Security and Communication Networks; 2021. p. 2021.
[23] Wang Y, Zhou G. The novel successive variational mode decomposition and weighted regularized extreme learning machine for fault diagnosis of automobile gearbox. Shock Vib 2021:2021.
[24] Kaveh A, Mahdavi VR. Colliding bodies optimization: a novel meta-heuristic method. Comput Struct 2014;139:18–27.